Proc. Natl. Acad. Sci. USA
Vol. 92, pp. 8463–8467, August 1995
Neurobiology

Oxidation of cysteine-322 in the repeat domain of microtubule-associated protein τ controls the *in vitro* assembly of paired helical filaments

(Alzheimer disease/neurofibrillary tangles)

OLAF SCHWEERS, EVA-MARIA MANDELKOW, JACEK BIERNAT, AND ECKHARD MANDELKOW

Max-Planck Unit for Structural Molecular Biology, c/o Deutsches Elektronen Synchroton, Notkestrasse 85, D-22603 Hamburg, Germany

Communicated by Donald L. D. Caspar, Florida State University, Tallahassee, FL, May 19, 1995 (received for review December 28, 1994)

ABSTRACT **One of the hallmarks of Alzheimer disease is the pathological aggregation of τ protein into paired helical filaments (PHFs) and neurofibrillary tangles. Here we describe the *in vitro* assembly of recombinant τ protein and constructs derived from it into PHFs. Though whole τ assembled poorly, constructs containing three internal repeats (corresponding to the fetal τ isoform) formed PHFs reproducibly. This ability depended on intermolecular disulfide bridges formed by the single Cys-322. Blocking the SH group, mutating Cys for Ala, or keeping τ in a reducing environment all inhibited assembly. With constructs derived from four-repeat τ (having the additional repeat no. 2 and a second Cys-291), PHF assembly was blocked because Cys-291 and Cys-322 interact within the molecule. PHF assembly was enabled again by mutating Cys-291 for Ala. The synthetic PHFs bound the dye thioflavin S used in Alzheimer disease diagnostics. The data imply that the redox potential in the neuron is crucial for PHF assembly, independently or in addition to pathological phosphorylation reactions.**

Several diseases are characterized by the pathological aggregation of a protein into fibers. This includes Alzheimer disease (AD), an age-related dementia. Brains of AD patients contain two types of deposits, the amyloid plaques and the neurofibrillary aggregates [tangles, paired helical filaments (PHFs)]. The former consists mainly of the proteins Aβ (the derivative of a membrane protein, APP); the latter consists of the microtubule-associated protein τ (reviewed in refs. 1 and 2). Analyzing the disease requires an understanding of the aggregation processes of these proteins. In the case of amyloid fibers the Aβ peptide self-associates by forming intermolecular interactions between β-pleated sheets. The fibers show a typical cross-β structure (3, 4), and they can be stained with dyes that are thought to interact preferentially with β-stranded proteins, such as Congo red or thioflavin S (5, 6).

The second hallmark of AD is the neurofibrillary tangles (NFTs) that consist of PHFs; they also stain with thioflavin S and (to a lesser extent) Congo red, thus suggesting a β substructure (6–8). In a previous study it was therefore unexpected to find that neither the fibers nor the subunit protein, τ, reveals secondary structure but rather behaves like a random-coil denatured protein (9). The observations suggest that the aggregation of τ is based on some principle other than β-strand interactions. In addition to aggregation, τ protein in AD is also extensively phosphorylated, especially at Ser-Pro motifs (review, ref. 10), and it has been suspected that this modification was related to the assembly into PHFs. Thus another unexpected finding was that PHFs can be reassembled *in vitro* from fragments of τ protein that lacked most of the phosphorylation sites and aggregated independently of phosphorylation (11). These studies also showed that the "repeat" domain of τ can form antiparallel dimers and that synthetic PHFs assemble from dimers that are chemically crosslinked with *N,N'*-phenylenedimaleimide (PDM) via sulfhydryls, implying that these links can be important in generating AD PHFs.

With these observations in mind, we initiated a study on the role of τ's sulfhydryl groups in PHF assembly and show here that the formation of synthetic PHFs depends on the intermolecular crossbridging of Cys-322. The results support the notion that an increase in the redox potential of aging neurons is responsible for the aggregation of PHFs, independently or in addition to the disequilibrium between protein kinases and phosphatases that leads to the concomitant hyperphosphorylation. Thus, the increase in redox potential and an excess protein oxidation found in aging brain (12) would provide a link for the aggregation of both types of AD fibers since the amyloid fibers also appear to be related to increased oxidation (13, 14).

MATERIALS AND METHODS

Preparation of Recombinant τ Protein. Constructs of τ protein were designed and expressed in *Escherichia coli* as described (15). They were based on the human τ isoforms provided by M. Goedert (16); the numbering of amino acids is that of the isoform htau40 containing 441 residues. The proteins were purified by Mono S FPLC ion-exchange chromatography with NaCl gradient. The protein purity was checked by SDS/PAGE.

Preparation of Synthetic PHFs. Prior to incubation, the proteins were dialyzed against 100 mM Tris (pH 6.8) to remove dithiothreitol (DTT) and concentrated by using a Centriprep (Amicon). The comparative assay was performed with the hanging-drop method for 7 days at 20°C. The well buffer contained 0.5 M Tris/1 M NaAc, pH 6.8. The protein concentrations were 5 mg/ml for K12 and K12A in 20 μl of 200 mM Tris/200 mM NaAc, pH 6.8. Similar experiments were made with K11 and the mutant K11 C291A (Cys-291 exchanged for an Ala). Large amounts of filaments were obtained with "batch" incubation of K12 under the same conditions [NaN_3 and phenylmethylsulfonyl fluoride (PMSF) added to 0.1 mM] for 1–6 weeks. These filaments were centrifuged for 1 hr at 82,000 × *g* at 4°C and resuspended in phosphate-buffered saline (PBS, pH 7) for fluorescence spectroscopy.

Preparation of AD PHFs. PHFs were isolated from brain tissues characterized for AD according to standard procedures. We employed the method of Greenberg and Davies (17), which results in the "soluble PHF" fraction. The PHF fraction was resuspended in PBS at pH 7 and centrifuged at

The publication costs of this article were defrayed in part by page charge payment. This article must therefore be hereby marked "*advertisement*" in accordance with 18 U.S.C. §1734 solely to indicate this fact.

Abbreviations: AD, Alzheimer disease; 2ME, 2-mercaptoethanol; DMSO, dimethyl sulfoxide; DTNB, 5,5'-dithiobis(2-nitrobenzoic acid); DTT, dithiothreitol; NFT, neurofibrillary tangle; PDM, *N,N'*-phenylenedimaleimide; PHF, paired helical filament; PMSF, phenylmethylsulfonyl fluoride.

36,000 rpm in a Beckman TST41.14 rotor for 1 hr at 20°C on a CsCl cushion (1.45 g/ml).

Electron Microscopy. For negative staining we used 600-mesh carbon-coated copper grids that were glow-discharged twice (CTA 010, Balzers Union). The grids were placed on a drop of protein solution, incubated for 5 sec, washed with two drops of water, placed on a drop of 2% uranyl acetate (pH 4.5), and incubated for 5 sec. The staining and washing solutions were first filtered through a 0.2-μm membrane. The replicas were examined in a Philips CM12 electron microscope at 100 kV.

Native Gel Electrophoresis of τ. Gel electrophoresis under native conditions was performed with 8% polyacrylamide gels with electrophoresis buffer containing 25 mM Mops and 50 mM L-histidine (pH 6.8) (18). Since K12 and K11 are basic, the proteins were electrophoresed toward the cathode. The number of free sulfhydryl groups was determined using 5,5′-dithiobis(2-nitrobenzoic acid) (DTNB) (19). DTT was taken as standard.

Fluorescence Spectroscopy. The labeling of sulfhydryls of K12 and K11 with pyrene was done in PBS (pH 8) at room temperature for 4 hr. The ratio of *N*-(1-pyrenyl)maleimide in dimethyl sulfoxide (DMSO) to protein was 10:1. The labeled proteins were purified from unreacted pyrene by gel filtration (PD10, Pharmacia). The concentrations of the proteins were 4.7 μM (K12) and 4.4 μM (K11). Protein concentrations were determined using the Bradford assay (Bio-Rad).

Concentrations of bound and free pyrene were measured spectroscopically at 342 nm using an extinction coefficient of 40,000 liter/(mol × cm). Free pyrene was determined in the supernatant after trichloroacetic acid precipitation. The concentrations were 0.5 μM (K12) and 0.65 μM (K11). The ratios of bound pyrene per cysteinyl were 0.52 (K12) and 0.4 (K11). Fluorescence-emission spectra of pyrene-labeled proteins were recorded on a Fluoromax single-photon counting fluorimeter (Instruments SA, Edison, NJ) over 370–560 nm with an excitation at 350 nm. Excitation band width was set at 1.25 nm; emission bandwidth was set at 0.8 nm. Fluorescence-emission spectra of thioflavin S were recorded with an excitation at 440 nm over a range of 455–600 nm (excitation and emission bandwidth, 1.125 nm). Protein concentrations were 0.3 mg/ml for a and c–e (Fig. 5). The thioflavin S (Sigma) concentration was 0.65 μM. The proteins without thioflavin S show no emission in the recorded range. The spectrum of thioflavin S as a blank is subtracted from each spectrum.

RESULTS

Interactions Between τ Molecules in Solution. For most of the experiments we chose recombinant htau23 (the smallest of the human τ isoforms; see ref. 16) or the constructs K12 and K11 diagramed in Fig. 1. The various isoforms of τ contained either three or four internal repeats. The repeat domain is implicated in the assembly of PHFs because it is found in the core of PHFs (20–22) and because τ constructs containing the repeats can assemble into PHF-like fibers *in vitro* (11). Four-repeat τ contains two Cys at positions 291 and 322; they are in the homologous KCGS motifs of the second and third repeat (Fig. 1). The second repeat may be absent due to alternative splicing so that three-repeat isoforms contain only one Cys (residue 322). Thus three-repeat τ can form disulfide bridges only between different molecules, whereas four-repeat isoforms can also have intramolecular bridges. During earlier experiments to generate τ dimers by PDM (a dual SH group crosslinker) we had already noticed that the three-repeat construct K12 crosslinks more efficiently with PDM than the four-repeat construct K11, suggesting that the two SH groups of K11 form intramolecular disulfide bridges and disable the molecule for dimerization. By the same token, when determining the accessible SH groups with DTNB, most SH groups were inaccessible in four-repeat isoforms or constructs, whereas they were accessible in three-repeat isoforms (data not shown). The interpretation of these experiments is hampered by the fact that SH group modifications and dimerization could not be observed simultaneously. We therefore sought a method that would be applicable to a solution of τ and would detect dimers with high sensitivity.

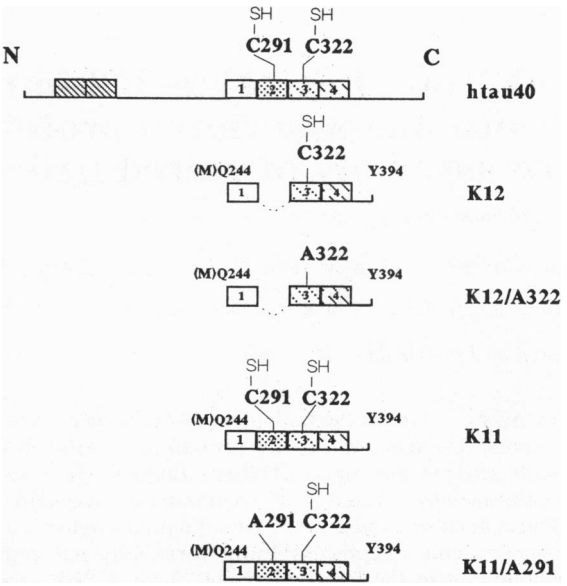

FIG. 1. Diagram of htau40, the largest human τ isoform in central nervous tissue (16), and related τ constructs. K12 (starting with Gln-244, ending with Tyr-394, without the second repeat Val-275 to Ser-305, M_r 13,079) contains repeats 1, 3, and 4 plus part of the C-terminal tail. Like all three-repeat isoforms, K12 contains only the single Cys-322. K12A is a point mutant where Cys-322 is exchanged for Ala. Construct K11 (M_r 16,326) is similar to K12 except that it has the additional second repeat and thus contains a second Cys at position 291.

We decided to label the sulfhydryls of τ and τ constructs with pyrene and to observe the fluorescence of the dye in solution. When excited at 350 nm, pyrene has an emission maximum at 393 nm. The quantum efficiency is strongly enhanced when pyrene becomes embedded in a hydrophobic environment; this provides a tool for observing protein–protein interactions such as actin assembly (23). Moreover, when two pyrene molecules approach one another to within 1 nm, they can form a joint excited state (excimer) that has a new emission maximum around 480 nm.

The behavior of labeled construct K11 (four repeats, two sulfhydryls) is shown in Fig. 2. It displayed a pronounced excimer fluorescence. By contrast, K12 (three repeats, one sulfhydryl) showed no or minimal excimer fluorescence. Both constructs had comparable intensities around the normal maximum at 393 nm. The results indicate that the pyrenes did not enter a more hydrophobic environment and that pairs of pyrenes approached each other in K11 but not in K12. At first sight one could conclude that K11 molecules interacted, bringing their pyrene moieties in close apposition, and that K12 molecules did not. However, in light of the experiments described below, another interpretation is appropriate: K11 folded over so that its two internal pyrenes formed an excimer state. In support of this, the excimer fluorescence did not increase with concentration (as would be expected of interacting molecules). K12, having only one pyrene on Cys-322, cannot form an intramolecular excimer. This result was surprising since K12 readily formed synthetic PHFs (see below). It becomes understandable when considering that sulfhydryls are necessary for aggregation, while in this experiment they were blocked by pyrene.

Sulfhydryl-Dependent Dimerization of τ. To assess the role of the sulfhydryls for aggregation we turned to native gel electrophoresis. In SDS/PAGE τ tended to oligomerize co-

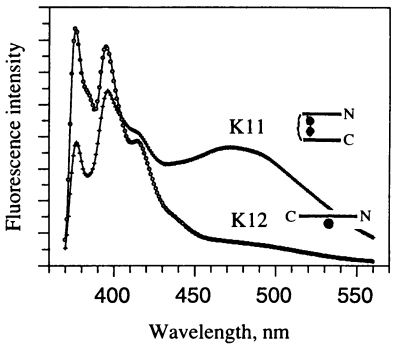

FIG. 2. Fluorescence-emission spectra of K12 (three repeats) and K11 (four repeats) labeled with pyrene at the SH groups; excitation wavelength is 350 nm. The labeling precludes the formation of disulfide bridges between τ molecules but would not prevent dimerization based on other interactions. The small arrowheads point to the emission maximum of pyrene in τ monomers at 393 nm. The wide maximum of the excimer state of pyrene (480 nm, caused by their close approach in dimers) is labeled with large arrowheads. Such excited pairs of pyrene are observed with K11 (containing the single Cys-322) but not with K12 (see *Insets*).

valently unless it is kept in a reduced state by DTT or 2-mercaptoethanol (2ME), and K12 is much more efficient than K11 in this regard. This behavior is much more evident in native gels (Fig. 3*A*). Lane 2 serves as a standard where construct K12 was in the presence of DTT, resulting in a purely monomeric population. When allowing this protein to stand without reducing agent it began to form mainly dimers, but also trimers, tetramers, and higher aggregates (Fig. 3*A*, lane 1). In contrast, the point mutant K12A (lacking the single Cys) remained monomeric (Fig. 3*A*, lane 3). This clearly shows that dimerization motifs other than disulfide linkage are not operating in τ. On the other hand, trimers and tetramers visible in lane 1 cannot all be stabilized by disulfide bridges because K12 contains only one Cys. Thus, it appears that the initial dimer formed by a disulfide bridge is a stable and necessary "template" for aggregation; this dimer has an antiparallel structure, as shown earlier (11). Once the dimer is formed, higher aggregates are stabilized by further contacts. The

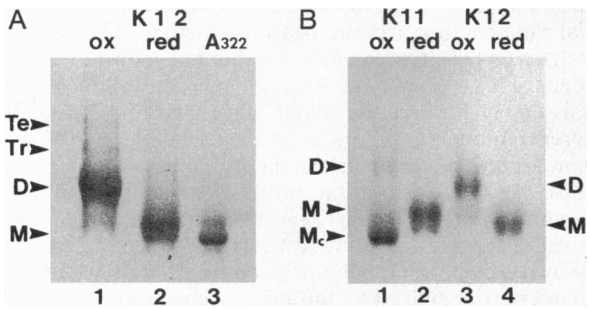

FIG. 3. (*A*) Native gel electrophoresis of K12 and K12A. Lane 1, K12 in nonreducing conditions; lane 2, K12 in reducing conditions (10 mM DTT). In DTT, τ is completely in the form of monomers (lane 2); in nonreducing conditions one observes dimers, trimers, tetramers, and higher oligomers, but no monomers (lane 1). Lane 3, K12A in nonreducing conditions; this protein occurs only as monomers and does not aggregate, even in the absence of DTT, indicating that the SH group of Cys-322 is necessary for aggregation. (*B*) Native gel electrophoresis of K12 and K11. Lane 1, K11 in nonreducing conditions. K11 forms mainly a monomer (M_c), which migrates faster than the K12 monomer and the extended K11 monomer (M), indicating a compact form. Lane 2, K11 in reducing conditions. Two populations of monomers are visible (M and M_c), an extended and a compact form. Lanes 3 and 4, K12 in nonreducing (lane 3) and reducing (lane 4) conditions. In lanes 1 and 3, <2% of the sulfhydryls are in the reduced state as determined with DTNB.

aggregates can be solubilized with lithium lauryl sulfate (2%), SDS (2%), guanidine hydrochloride (2 M), and 2ME (20%) (1 hr, 20°C). In contrast to K12, K11 forms only a minor population of dimers in the oxidized form (Fig. 3*B*, lane 1). Less than 2% of the sulfhydryls of K11 (lane 1) and K12 (lane 3) were in a reduced state, as determined with DTNB. Interestingly, the K11 oxidized monomer (M_c) migrates faster than in the reduced state (M, lane 2), indicating a more compact form due to the intramolecular S—S bridge.

Assembly of PHFs *in Vitro*. The above sets of experiments suggested that the repeat domain of τ could interact via its sulfhydryls and that the interaction was prevented either by mutating the Cys (as in construct K12A) or by blocking it (for example, with pyrene). We therefore generated monomeric τ with free SH groups, incubated for prolonged periods in crystallization-like conditions (hanging drop), and observed the products by negative-stain electron microscopy. As the reducing power of the initial 2ME gradually disappears, the protein molecules are able to react with one another. Fig. 4*A* shows that K12 forms a dense network of filaments, which at higher power reveal the characteristic PHF structure (≈75-nm crossover repeat, width between 10 and 20 nm, Fig. 4*B*). Many of the filaments have the short "bow-tie"-like appearance typical of the "soluble PHF fraction" from AD brains (17). The fibers can be pelleted and concentrated (Fig. 4*A*). However, when the same experiments are performed with the SH-less construct K12A (Fig. 4*C*), no fibrils are observed. These data argue strongly that Cys-322 of τ is essential for the formation of PHFs. We note that the experiments were done with a recombinant τ construct (K12, the repeat domain) free of phosphorylation.

In contrast to the three-repeat construct K12, the four-repeat construct K11 aggregated much less readily, and *bona fide* PHFs were not observed. This correlates with the lower tendency of K11 for oligomerization seen in the native gels. It appears that the additional repeat inhibits intermolecular interactions, either by stabilizing a distinct conformation or by allowing Cys-322 in the third repeat to become internally blocked by a disulfide linkage with Cys-291 in the second repeat (Fig. 3*B*, lane 1), thus making it unavailable for crosslinking with another molecule. This possibility would be consistent with the close approach of the two cysteines visible by the excimer fluorescence (Fig. 2). If Cys-291 is mutated for Ala in K11, the mutant construct aggregated readily into fibrils (Fig. 4*D*). Full-length τ isoforms such as htau23 (three repeats) or others could not be assembled reproducibly into PHFs *in vitro*. As noted earlier (24), most τ variants do aggregate with time, either in the form of undefined deposits or even into filamentous forms, but these do not normally show the characteristic features of PHFs so that the relationship between these structures and PHFs remains undefined.

Reactions of PHFs with the Diagnostic Dye Thioflavin S. Thioflavin S absorbs light in the near-UV and thus gives the stained structures a yellow color. It fluoresces when excited at 440 nm and shows an emission maximum at 480–490 nm (6). In solution, synthetic PHFs made from construct K12 and natural PHFs prepared from AD tissue show the expected fluorescence, whereas nonaggregated solutions of K12, dimers of K12 chemically crosslinked by PDM, or the point mutant K12A show negligible fluorescence at the same total protein concentration (Fig. 5). These experiments allow two conclusions: (*i*) the synthetic PHFs indeed resemble the natural ones in terms of thioflavin S fluorescence and thus reinforce the similarity of these structures and (*ii*) the fluorescence is linked to the assembled state. This feature provides a sensitive tool for monitoring the self-assembly of PHFs.

DISCUSSION

τ is a protein with a hydrophilic character that is normally highly soluble. Its physiological role is presumably to stabilize

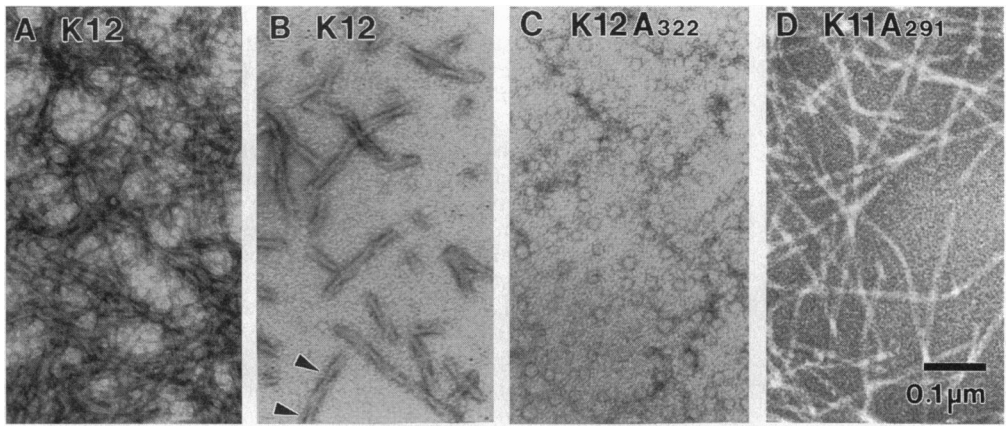

FIG. 4. Electron micrographs of PHFs formed from K12. (*A*) Pelleted filaments. (*B*) Filaments showing the typical PHF structure with crossover repeats around 75 nm and widths between 10 and 20 nm. (*C*) $K12A_{322}$: no filaments are formed by this construct. (*D*) Filaments formed from K11 with Cys-291 mutated for Ala.

microtubules in axons and thus to lay the groundwork for the microtubule-based axonal transport. In considering the pathological consequences of τ aggregation in AD, two aspects seem to be important. (*i*) If AD τ is modified (e.g., by phosphorylation) so that it no longer binds to microtubules, they could break down and interrupt axoplasmic flow. (*ii*) Aggregated τ could obstruct the cell and thereby cause its death. It is therefore important to find out how τ interacts with microtubules, how it is phosphorylated, and how it aggregates.

τ is easily phosphorylated by many kinases, and certain phosphorylation reactions, particularly at Ser-262 in the first repeat, can indeed cause the detachment of τ from microtubules under the influence of certain kinases such as MARK (25, 26). However, the aggregation of τ has remained enigmatic for several reasons. *In vitro*, it has been very difficult to assemble *bona fide* PHF-like filaments from τ preparations or from recombinant τ isoforms (11, 27), in contrast to certain τ constructs that assemble with relative ease, as shown here for K12. Second, it is not clear whether there is a role for phosphorylation in assembly. We therefore decided to focus our attention first on the assembly properties of the different τ isoforms and constructs, independently of phosphorylation. The main results of this study can be summarized as follows:

(*i*) τ constructs containing three repeats (e.g., K12) have a high tendency to form oligomers and polymers, in contrast to whole τ, or constructs containing four repeats (Figs. 3 and 4).

(*ii*) The dimerization and polymerization of the three-repeat constructs depend on the capacity of Cys-322 to form intermolecular disulfide bridges. If Cys-322 is mutated, assembly of synthetic PHFs is inhibited.

(*iii*) In the case of four-repeat constructs (e.g., K11), repeats 2 and 3 are folded such that the two cysteines (Cys-291 and Cys-322) come into close contact, indicating a potential for intramolecular disulfide bridging (rather than intermolecular). If Cys-291 is mutated for Ala, the ability to form synthetic PHFs is regained. This would explain the poor assembly of the four-repeat construct.

(*iv*) Thioflavin S, a widely used stain for diagnosing AD deposits, stains synthetic PHFs as well (but not the unpolymerized subunits), attesting to the similarities between native and synthetic PHFs (Fig. 5).

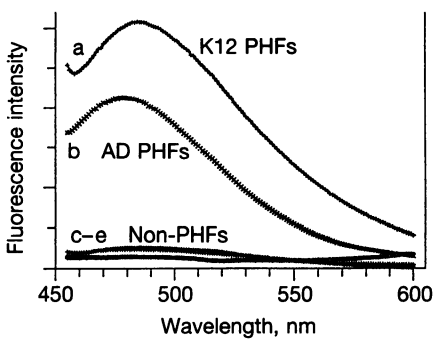

FIG. 5. Thioflavin S fluorescence of synthetic and natural PHFs. Excitation wavelength is 440 nm; emission maximum is in the 485-nm range. Spectrum a, PHFs formed from recombinant K12; spectrum b, PHFs prepared from AD brain tissue. Both types of fibers can be detected by thioflavin S fluorescence. Spectrum c, K12 monomers; spectrum d, K12 dimers crosslinked with PDM; spectrum e, K12A. These nonfilamentous particles do not show thioflavin S fluorescence.

What do these results tell us about the assembly of PHFs? First, in our hands the assembly of any of the full-length τ isoforms into PHFs is inefficient so that one has to assume that the domain required for the PHF-like interaction is blocked, say by the N- or C-terminal flanking regions, or that intact τ has a different conformation. Intact τ does form fibrous aggregates in some conditions (e.g., refs. 24, 27, and 28), but the structural relationships to PHFs are not clear. Among the different domains of τ protein, the repeat domain is clearly the important one for PHF assembly. This agrees well with the observation that the core of AD PHFs contains the repeat domain (20, 21, 29). In particular, the minimal protease-resistant unit of AD PHFs comprises the equivalent of three repeats (22), and these closely resemble the construct K12.

The repeats are necessary for assembling PHFs "*in vitro*," but are they sufficient? The answer appears to be negative: apart from the repeats as such, a SH group in repeat 3 has to be available for forming intermolecular disulfide linkages. This initial dimerization was the basis for further PHF assembly. Constructs whose dimerization is inhibited show no tendency to form PHFs (e.g., K11 or K12A). However, this implies that the assembly beyond the dimer stage must be based on a different interaction, both from a structural and from a chemical point of view (Fig. 6): the K12 dimer has no free SH groups, so that association of the next molecules (be it monomers, dimers, or other) must be possible independently of disulfide bridges. This could be based on a new conformation instead of the flexible, "denatured" conformation of monomeric τ stabilized by the initial dimerization. Note that the native gels show higher oligomers only in conditions where the initial dimer is also prominent (Fig. 3). Effectively the results described here deal with the conditions for nucleation of the filaments in a simplified, *in vitro* system; little is known at present about the further elongation, other than the fact that nucleation is a necessary first step. However, in AD the initial nucleation might well be the crucial step and the seed could function as a "pathological chaperone;" this would make PHF assembly similar to a model currently discussed for the seeded assembly of amyloid fibers (30).

The possible relationship between the redox state of the cell and the degeneration in AD has attracted increasing attention in recent years (e.g., refs. 12 and 14). Aging cells have an impaired activity of mitochondrial enzymes of the respiratory chain due to accumulating damage to the mitochondrial genes

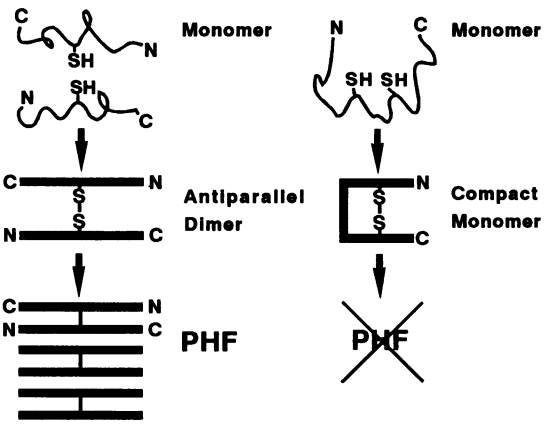

FIG. 6. Model of the aggregation of PHFs. The essential first step is the dimerization of τ via the formation of disulfide bridges; the molecules in the dimers are arranged in an antiparallel fashion (11). This serves as a template for further elongation by dimers. The latter process probably does not depend on disulfide bridge formation because the single Cys residues are already bound up by formation of dimers (pathway on left). Constructs with two Cys form compact monomers but cannot nucleate PHFs.

(31, 32). The resulting increase in redox potential may have many effects, including a reduced level of reduced glutathione. Once the balance between reduced and oxidized glutathione is perturbed, there is a chance that intracellular SH groups (which should normally remain in a reduced state) react with each other to form disulfide bridges. If this leads to aggregates where the links are shielded from the cytosol, the process could become essentially irreversible. Such unphysiological aggregates should normally be degraded by cytosolic proteases or refolded by chaperones. However, this system might itself be impaired due to oxidative damage, and, in addition, the hyperphosphorylation of τ in AD might contribute its share toward making PHFs undigestible (33, 34). Interestingly, the cytotoxicity of amyloid peptide Aβ is accompanied by an impaired reducing power (13, 14).

In the same context it is notable that the E4 isoform of apolipoprotein E correlates with an increased risk for AD; this isoform differs from the others by having no cysteines, and this could be responsible for a difference in its binding to τ protein and microtubules (35). This feature would therefore also point to a role of oxidation of proteins in AD, independently of other effects caused by phosphorylation.

At this point, there appear to be two residues in τ protein that are of key importance for switching τ between different states: Ser-262 in the first repeat and Cys-322 in the third. Ser-262 can be phosphorylated, in particular by kinases such as MARK, and this leads to the detachment of τ from microtubules (25, 26), thus setting it free for further self-assembly. Significantly, Ser-262 shows pronounced phosphorylation in AD (36). On the other hand, Cys-322 can be oxidized, and this leads to PHF assembly (ref. 11; this report). *In vitro* this is achieved most easily by using constructs of the "fetal" isoform of τ (htau23) that has only three repeats. Conversely, reducing agents or the second repeat or τ can be viewed as "antidotes" against PHF assembly.

We thank N. Burmester for excellent technical assistance. AD brain tissue was kindly provided by the Bryan Alzheimer Center at Duke University (Durham, NC), the Alzheimer Center at the University of Rochester (Rochester, NY), and the Brain Tissue Resource Center at McLean Hospital, Harvard Medical School (Belmont, MA). This work was supported by grants from the Deutsche Forschungsgemeinschaft and the Bundesministerium für Forschung and Technologie. This study contains part of the doctoral thesis of O.S.

1. Anderton, B. H. (1993) *Hippocampus* **3,** 227–237.
2. Trojanowski, J. Q. & Lee, V. M. Y. (1994) *Am. J. Pathol.* **144,** 449–453.
3. Kirschner, D. A., Abraham, C. & Selkoe, D. J. (1986) *Proc. Natl. Acad. Sci. USA* **83,** 503–507.
4. Inouye, H., Fraser, P. E. & Kirschner, D. A. (1993) *Biophys. J.* **64,** 502–519.
5. Glenner, G. G., Eanes, E. D. & Page, D. L. (1972) *J. Histochem. Cytochem.* **20,** 821–826.
6. LeVine, H. (1993) *Protein Sci.* **2,** 404–410.
7. Wisniewski, H. M., Wen, G. Y. & Kim, K. S. (1989) *Acta Neuropathol.* **78,** 22–27.
8. Hyman, B., Van Hoesen, G., Beyreuther, K. & Masters, C. (1989) *Neurosci. Lett.* **101,** 352–355.
9. Schweers, O., Schönbrunn-Hanebeck, E., Marx, A. & Mandelkow, E. (1994) *J. Biol. Chem.* **269,** 24290–24297.
10. Mandelkow, E.-M. & Mandelkow, E. (1993) *Trends Biochem. Sci.* **18,** 480–483.
11. Wille, H., Drewes, G., Biernat, J., Mandelkow, E.-M. & Mandelkow, E. (1992) *J. Cell Biol.* **118,** 573–584.
12. Smith, C. D., Carney, J. M., Starke-Reed, P. E., Oliver, C. N., Stadtman, E. R., Floyd, R. A. & Markesbery, W. R. (1991) *Proc. Natl. Acad. Sci. USA* **88,** 10540–10543.
13. Shearman, M. S., Ragan, C. I. & Iversen, L. L. (1994) *Proc. Natl. Acad. Sci. USA* **91,** 1470–1474.
14. Behl, C., Davis, J. B., Lesley, R. & Schubert, D. (1994) *Cell* **77,** 817–827.
15. Biernat, J., Mandelkow, E.-M., Schröter, C., Lichtenberg-Kraag, B., Steiner, B., Berling, B., Meyer, H. E., Mercken, M., Vandermeeren, A., Goedert, M. & Mandelkow, E. (1992) *EMBO J.* **11,** 1593–1597.
16. Goedert, M., Spillantini, M., Jakes, R., Rutherford, D. & Crowther, R. A. (1989) *Neuron* **3,** 519–526.
17. Greenberg, S. G. & Davies, P. (1990) *Proc. Natl. Acad. Sci. USA* **87,** 5827–5831.
18. Guttmann, R., Erickson, A. C. & Johnson, G. V. W. (1995) *J. Neurochem.* **64,** 1209–1215.
19. Ellman, G. L. (1959) *Arch. Biochem. Biophys.* **82,** 70–77.
20. Kondo, J., Honda, T., Mori, H., Hamada, Y., Miura, R., Ogawara, M. & Ihara, Y. (1988) *Neuron* **1,** 827–834.
21. Wischik, C., Novak, M., Thogersen, H., Edwards, P., Runswick, M., Jakes, R., Walker, J., Milstein, C., Roth, M. & Klug, A. (1988) *Proc. Natl. Acad. Sci. USA* **85,** 4506–4510.
22. Novak, M., Kabat, J. & Wischik, C. M. (1993) *EMBO J.* **12,** 365–370.
23. Kouyama, T. & Mihashi, K. (1981) *Eur. J. Biochem.* **114,** 33–38.
24. Lichtenberg-Kraag, B. & Mandelkow, E.-M. (1990) *J. Struct. Biol.* **105,** 46–53.
25. Biernat, J., Gustke, N., Drewes, G., Mandelkow, E.-M. & Mandelkow, E. (1993) *Neuron* **11,** 153–163.
26. Drewes, G., Trinczek, B., Illenberger, S., Biernat, J., Schmitt-Ulms, G., Meyer, H. E., Mandelkow, E.-M. & Mandelkow, E. (1995) *J. Biol. Chem.* **270,** 7679–7688.
27. Crowther, R. A., Olesen, O. F., Smith, M. J., Jakes, R. & Goedert, M. (1994) *FEBS Lett.* **337,** 135–138.
28. Degarcini, E. M., Carrascosa, J. L., Nieto, A. & Avila, J. (1990) *J. Struct. Biol.* **103,** 34–39.
29. Ksiezak-Reding, H. & Yen, S. H. (1991) *Neuron* **6,** 717–728.
30. Jarrett, J. T. & Lansbury, P. T. (1993) *Cell* **73,** 1055–1058.
31. Wolvetang, E. J., Johnson, K. L., Krauer, K., Ralph, S. J. & Linnane, A. (1994) *FEBS Lett.* **339,** 40–44.
32. Shigenaga, M. K., Hagen, T. M. & Ames, B. N. (1994) *Proc. Natl. Acad. Sci. USA* **91,** 10771–10778.
33. Litersky, J. M. & Johnson, G. V. W. (1992) *J. Biol. Chem.* **267,** 1563–1568.
34. Morishima-Kawashima, M., Hasegawa, M., Takio, K., Suzuki, M., Titani, K. & Ihara, Y. (1993) *Neuron* **10,** 1151–1160.
35. Strittmatter, W. J., Weisgraber, K. H., Goedert, M., Saunders, A. M., Huang, D., Corder, E. H., Dong, L. M., Jakes, R., Alberts, M. J., Gilbert, J. R., Han, S. H., Hulette, C., Einstein, G., Schmechel, D., Pericak-Vance, M. & Roses, A. (1994) *Exp. Neurol.* **125,** 163–171.
36. Hasegawa, M., Morishima-Kawashima, M., Takio, K., Suzuki, M., Titani, K. & Ihara, Y. (1992) *J. Biol. Chem.* **267,** 17047–17054.